6-1-2018

Mass Accretion and Ozone Reactivity of Idealized Indoor Surfaces in Mechanically or Naturally Ventilated Indoor Environments

Elliott Gall
Portland State University, gall@pdx.edu

Donghyun Rim
Pennsylvania State University

Citation Details

Gall, E. T., & Rim, D. (2018). Mass accretion and ozone reactivity of idealized indoor surfaces in mechanically or naturally ventilated indoor environments. Building and Environment, 138, 89-97.

Mass accretion and ozone reactivity of idealized indoor surfaces in mechanically or naturally ventilated indoor environments

Elliott T. Gall[1,2], Donghyun Rim[3]

[1]Mechanical and Materials Engineering, Portland State University, Portland, OR 97201, USA
[2]Nanyang Technological University and Berkeley Education Alliance for Research in Singapore, Singapore 138602
[3]Architectural Engineering Department, Pennsylvania State University, University Park, PA 16802, USA

[*]Corresponding author: Elliott T. Gall
Email: gall@pdx.edu

Abstract

In indoor environments, accretion of mass to materials may provide sites for surface chemistry that differ from those of the original material. Since indoor surfaces are a major sink of oxidant gases, surface mass accretion may impact indoor O_3 chemistry. In this study, the effect of surface mass accretion on O_3 surface deposition was tested by deploying cleaned borosilicate glass plates in two types of indoor environments: a mechanically ventilated (MV) office and a naturally ventilated (NV) residence located in Singapore. In each environment, seven replicate glass plates and one field blank were deployed for between 7-56 days and examined in a laboratory chamber for O_3 deposition rate and surface reaction probability. Average mass accretion to plates, deployed in a horizontal position and including deposited particles, was 10.6 mg/(m^2 d) in the MV office vs. 18.5 mg/(m^2 d) in the NV residence and the comparison is at the threshold of statistical significance (p = 0.054). Ozone reactivity to the plates increased in magnitude and persistence with longer plate deployment. Ozone reaction probabilities to cleaned plates prior to deployment ranged [0.06-0.74]×10^{-6} for two hours of observable removal whereas plates deployed for 56 days ranged [0.15-1.2]×10^{-6} for four hours of observable removal. Regressions of cumulative O_3 removed during chamber tests vs. mass accreted show removal of 4.3 nmol O_3/mg for the NV residence and 2.4 nmol O_3/mg for the MV office. These results imply that accretion of mass to surfaces may alter indoor O_3 transport and transformation pathways.

1 Introduction

Exposure to elevated O_3 is associated with cardiovascular effects, asthma, and increases in daily mortality [1–3]. Humans are exposed to O_3 primarily in the small fraction of the atmosphere contained inside built environments. The predominant source of indoor O_3 is from outdoor air where O_3 is formed due to photochemical reactions that involve sunlight, volatile organic compounds (VOCs), NO_x, and carbon monoxide [4]. Indoor O_3 levels are 20-70% that of outdoor levels mainly due to chemical reactions with interior surfaces that remove O_3 from air [5]. In spite of lower indoor O_3 levels, total indoor O_3 exposures typically exceed outdoor exposures because of the time spent in indoors [6–8]. Epidemiological studies suggest a safe level of exposure to O_3 is below 10 ppb [9], a level which indoor spaces routinely exceed

[5]. Certain surface O_3 reaction pathways may generate byproducts, effectively trading indoor O_3 for other harmful or irritating byproducts [10]. There is interest in developing beneficial indoor surface O_3 pathways to passively reduce human exposure to O_3, if removal results in no byproducts or only benign byproducts [11,12].

In a typical indoor space, many exposed surfaces can react with O_3. A seminal study of indoor O_3 dynamics reported ozone decay constants for homes and decomposition rates for specific indoor surfaces [13]. Subsequent studies have expanded our knowledge of indoor O_3 dynamics by characterizing reaction rates with a wide variety of building materials [11,12,14–22], as well as identifying byproduct formed from material-O_3 reactions [10,23–26]. Outcomes of studies of material-O_3 interactions generally report material reactivity as a deposition velocity, v_d [27], or a reaction probability, γ [28]. Such parameterizations enable material balance models of indoor O_3 that describe fate, transport, and transformation of O_3 and O_3 reaction byproducts [16,29–31].

As materials react with O_3, so-called "aging" phenomena are observed where ozone reactivity decreases with time. Over short time-scales (< 10 h), this has been observed in chamber tests where materials are exposed to elevated O_3 that is alternated with air free of O_3 on a time scale of hours [13]. Under such conditions, materials generally exhibit a reduction in material-O_3 reactivity with increasing exposures or exposure periods [14,18,21]. This behavior is ascribed to exhaustion of reaction sites on the surface after initial O_3 exposure, with subsequent O_3 removal rate-limited by diffusion of new reaction sites to the surface [32].

Over longer time-scales, e.g., months of deployment in real buildings, prior studies demonstrate variability in impacts on magnitudes of material-O_3 reactivity. In a study where four materials were placed in field sites over a period of ~6 months, material-O_3 v_d increased modestly for ceiling tile, decreased for carpet, and was largely unchanged for activated carbon and painted drywall [25]. Another study of material-O_3 reaction showed that for three building materials deployed in an occupied office environment, v_d decreased for painted drywall after 1 and 2 months of deployment while v_d for carpet and

63 ceiling tile decreased after 1 month, subsequently increasing to higher than the “fresh” reactivity after 2
64 months of placement in the field [18]. These studies posit that deposition processes occurring in the
65 indoor environment provide a mechanism by which gases and particles may associate with the surface, in
66 some cases replenishing O_3 surface reaction sites.

67 Accretion of low-volatility gases, particles, water, inorganic species and elemental carbon create a surface
68 film on indoor surfaces [33]. Previous studies show that sorption of low-volatility compounds and
69 deposition of particles impact the chemical composition of building and indoor surfaces. Studies of indoor
70 and exterior window surfaces demonstrate that window surfaces act as a reservoir for alkanes, polycyclic
71 aromatic hydrocarbons, polychlorinated biphenols, and pesticides [34,35]. Another study investigated
72 surface film formation by heating glass and aluminum materials that were initially clean and then exposed
73 to successively longer periods of an indoor air matrix [36]. Time exposed to indoor air was a strong
74 determinant of ultrafine particle formation, due to condensation of SVOCs that were volatilized from the
75 material during a controlled heating process. Settling of indoor dust may also alter surface chemical
76 composition. A study of the O_3 reactivity of indoor dust shows high rates of O_3 removal to dust, with
77 increases of C_7-C_9 aldehydes and other reaction byproducts produced from O_3-dust reactions [32].

78 Given the importance of indoor surfaces in governing indoor O_3 and O_3 reaction byproduct
79 concentrations, the objective of the present study is to investigate dynamics of surface mass accretion and
80 the resulting reactivity of indoor surfaces. This study addresses this knowledge gap by measuring how
81 surface film accretion impacts ozone deposition and surface reaction probability. While other studies have
82 explored this phenomena, this work uses glass plates as an idealized surface that reduces confounders
83 such as initial material composition, material aging, and material cleanliness in subsequent studies of
84 accreted mass. However, glass is also a common indoor material such that mass accretion can be taken as
85 representative of what can occur on certain surfaces in real indoor environments. The study results will
86 provide baseline data for how mass is accreted to initially inert, clean materials and subsequent ozone-

surface reaction dynamics in two typical indoor environments: 1) a naturally ventilated residence and 2) a mechanically ventilated office.

2 Methods

2.1 Glass plates

Borosilicate glass plates were selected as surfaces to facilitate investigations of the dynamics of the mass accumulated to indoor surfaces (i.e., a surface film of deposited particles and/or sorbed gases from indoor air) and resulting ozone reactivity of the glass plate/surface film. Borosilicate glass plates were selected due to the inertness and smoothness of glass and the known low uptake of O_3 to clean glass [19,30]. Glass provides a low baseline from which subsequent signals of O_3 uptake to accreted masses can be more readily differentiated. Borosilicate glass plates (McMaster-Carr) with horizontal projected surface area of 232 cm^2 (15.24 cm × 15.24 cm, thickness = 0.3175 cm) were used in this investigation.

Prior to deployment in the field, sixteen glass plates were cleaned by washing with laboratory-grade soap and a soft sponge. All glass plates were then rinsed in water three times to ensure no soap film remained. Glass plates were then cleaned with a lint-free wipe (Kimtech Kimwipes, Kimberly-Clark Professional) dipped in high purity isopropyl alcohol (Levinson Scientific and Chemicals, IPA Technical Grade >99%) and allowed to air dry in a fume hood in a vertical position. After drying, all plates were heated with a heat gun for fifteen minutes to vaporize remaining solvent or other sorbed volatile species. All plates were then placed in a chamber apparatus (details in Section 2.4) and were passivated of ozone reaction sites by supplying approximately 500 ppb of ozone to the chamber for 8 h. All plates were then immediately weighed (see section 2.3) to obtain the initial mass of the plate and placed in polypropylene storage bags for ~1 week until deployment into the field environments. Tests of O_3 reactivity were made for two randomly selected plates to establish a baseline ozone deposition velocity (v_d) to a clean plate.

2.2 Deployment and collection of glass plates

Seven test plates and one field blank plate were randomly selected from the set of sixteen plates for concurrent deployment to two indoor environments: a naturally ventilated (NV) residential dwelling and a

mechanically ventilated (MV) office building. In both environments, the seven plates were placed on wire racks such that the plates were horizontal to the ground (see Fig. S1 for an image of the deployment). A field blank, a glass plate prepared as described in Section 2.1, but deployed to the field environment in the polypropylene bag, was deployed to each of the field locations. In both locations, the temperature (°C), relative humidity (%), and light (lux) levels were recorded in 5-minute interval (HOBO U12-012, Onset Computer Corporation), shown in Fig. S2. In both the MV and NV location, plates were deployed for a total of 56 days. Test glass plates were collected at approximately weekly intervals while a field blank was collected after deployment for three weeks (NV residence) and eight weeks (MV office).

Racks used to support glass plates were placed in unobtrusive locations that were representative of typical tabletop height surfaces in each environment. Racks were used to facilitate testing of ozone removal to the downward facing side of the plate subsequent to the upward face. However, no observable O_3 removal could be discerned to the downward facing plate. Results presented here are tests where only the upward facing side of the plate was exposed to O_3 inside the chamber. In the MV office building, the wire racks with plates were placed on a desk height table top, typical of an office environment where computer-related work tasks are conducted. The office building is served by a demand-controlled ventilation system that introduces outdoor air proportional to the amount of carbon dioxide in the space, and includes mechanical systems for filtration (MERV 6-8 rated filters), cooling, and dehumidification. The ventilation rate was not measured during the period of the deployment. The plates were placed on an L-shaped desk, approximately 1 m in distance from the workstation where an office worker was present during normal working hours. The zone was typically occupied by 5-15 office workers.

In the NV residential environment, the racks with the seven test plates and one field blank were placed on a television stand in a living room at approximately 1 m in height. The residential environment was occupied by two individuals, typically during non-working hours. The zone the plates were placed in was served only by fan-assisted natural ventilation; ventilation and cooling were provided to the space by window opening and fans that were operated to draw outdoor air into the room based on the preference of

137 the occupants. The typical schedule was windows closed with fans off during working hours, windows
138 open with fans on during evenings and weekends, and windows closed with fans off during sleeping
139 hours. The ventilation rate was not measured during the period of the deployment.

140 The two sites investigated were located within 1 km of each other in vicinity of the National University of
141 Singapore and we expect the outdoor conditions to be similar. We lack accompanying air quality data at
142 the field sites; in general, the Singapore National Environment Association reported Pollutant Standard
143 Index levels of 30-50 across the period of this study, indicating "good" to "moderate" outdoor air quality.
144 In such conditions, indoor particle and ozone concentrations are likely higher for the naturally ventilated
145 residence than the mechanically ventilated office because of no filtration with frequently open windows in
146 the residence. The MV and NV location were approximately a 5 min and 15 min walk, respectively, from
147 the laboratory where analyses occurred. The protocol developed for transporting plates for analysis
148 consisted of wearing new nitrile gloves to carefully place plates into polypropylene bags sized such that
149 there was no contact between the top surface of the plate and the bag. The plate was then placed in a
150 container to be immediately transported, in the same orientation as when placed in the field, to the
151 laboratory for weighing and analysis of ozone removal. It took less than two hours until the samples were
152 analyzed in the laboratory.

153 **2.3 Measurement of mass accretion to glass plates**

154 Initial plate mass was measured with an analytical balance (ME204, Mettler Toledo), with an absolute
155 uncertainty of ±0.0001 g. While plates were nominally of uniform dimension and material, each plate was
156 tracked specifically as small variations in initial plate mass were noted (μ = 170.1751 g, σ = 0.44 g). After
157 deployment to the field and subsequent return to the laboratory, each plate was measured by placing the
158 plate on a clean sheet of weighing paper and allowing the mass reading to stabilize over a period of
159 approximately 1 min and the change in mass from its initial "clean" measurement was noted. The
160 environmental conditions of the laboratory were different from that of both the MV office environment
161 and the NV residence. The 1 min duration was chosen to allow the reading to stabilize from the

disturbance of placement of the plate onto the scale, but to preclude longer-duration phenomena such as the equilibration of sorbed water with the laboratory environment.

Average mass accretion rates to the plates deployed in the field were calculated according to eq. 1:

$$\dot{m} = \frac{(m_f - m_i)}{t_d A} \quad (1)$$

where $\dot{m}$ is the mass accretion rate to a test plate (g/(m^2 d)), m_f is the final mass accreted to a test plate after a field deployment (g), $m_{,i}$ is the initial mass of a cleaned plate prior to deployment (g), t_d is the time duration the plate spent deployed in the field (d), and A is the exposed area of the top surface of the plate (m^2). Since the bottom surface was also exposed to the environment, the normalization introduces a small error as some mass may have accumulated on the bottom surface. The implications of this assumption are discussed in Section 3.1.

2.4 Test apparatus

Ozone deposition velocities were measured in a laboratory chamber apparatus; a schematic of the apparatus is shown in Fig. 1. Compressed laboratory air passed through a membrane dryer that included a 0.1 micron pre-filter (Laman MD-15LS and Laman SAM350-E, Air Parts Center Pte Ltd) to remove particles and water vapor present in the compressed air. Dried, particle-free air was then passed through a packed bed of activated carbon (BPL 6×16, Calgon Carbon) to remove ozone and volatile organic compounds. The air flow was then split into three streams with flow rates set and maintained using mass flow controllers (Omega FMA5500, Omega Singapore). One stream was used to humidify the airflow to the desired setpoint based on the depth of deionized water in the water column and the flowrate through the column. The second stream was an unmodified flow of dry, clean air that was mixed with the humidified stream to maintain the desired relative humidimty (RH) set-point. The third stream passed through a stable ozone generator (U04/97-0066-02, UVP LLC). These three flow streams were re-combined prior to entering a temperature controlled enclosure (KBE3.1, Binder GmBH) that was used to

maintain the air temperature and humidity to constant setpoints. Inside the temperature controlled enclosure was an 11.4 L electropolished stainless steel chamber (CTH-24, Eagle Stainless) in which glass plates were placed. A sensor was placed in an outlet stream from the test chamber to measure the chamber temperature and RH (U12-012, Onset Computer Corporation).

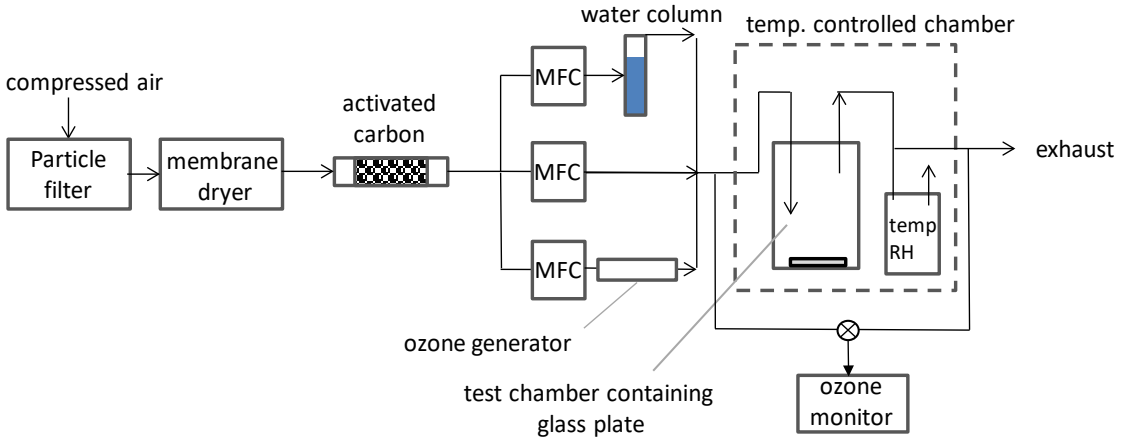

Fig. 1. Schematic of test apparatus for measuring ozone deposition occurring on clean and field deployed glass surfaces. MFC = mass flow controller, RH = relative humidity.

2.5 Experimental protocol

Prior to a test of a glass plate, a test of background O_3 removal of the empty stainless steel chamber was conducted. Ozone was injected into the empty chamber at a stable until steady-state conditions, defined as changing less than 2 ppb in a 20 minute time period [37]. After conducting a background test of an empty chamber, a cleaned (week 0), field-environment deployed plate (weeks 1-7), or field blank glass plate was placed in the chamber and the O_3 injection was repeated. Ozone injections when glass plates were present were conducted for a period of four hours; longer test durations were explored but resulted in deposition velocities that were indistinguishable from background removal. A switching valve was used to periodically alternate between inlet and outlet concentrations of ozone (Model 202, 2BTech). Across all experiments, the average (mean ± 1 std. dev.) temperature and RH was 25.2 ± 0.057 °C and 49.3 ± 1.8%. Experiments were conducted with an average chamber flowrate of 2.2 ± 0.1 L/min (air exchange rate = 11.5 /h). Inlet ozone concentrations to the test chamber were an average 96.8 ± 2.0 ppb.

2.6 Data analysis

2.6.1 Determination of v_d, v_t, γ

The background loss rate L_{bg} (h^{-1}) of ozone was calculated from steady-state data according to eq. 2:

$$\frac{dC_{outlet}}{dt} = 0 = \lambda C_{inlet} - \lambda\, C_{outlet} - L_{bg}\, C_{outlet} \quad (2)$$

where C_{inlet} and C_{outlet} are the inlet and outlet concentrations of ozone (ppb), t is time (h), λ is the air exchange rate (h^{-1}) and L_{bg} is the background loss rate (h^{-1}) to stainless steel chamber surfaces. Ozone v_d to background chamber stainless steel surfaces were calculated using the exposed area of the stainless steel chamber surfaces (1810 cm^2) and the chamber volume (11,400 cm^3). Ozone v_d to stainless steel surfaces were, on average, ~0.002 cm s^{-1} and was determined in a background test prior to each experiment. Ozone deposition velocity (v_d) to glass plates was determined using a transient mass balance relationship that was solved numerically for the deposition velocity in 5-min interval, as shown in eq. 3:

$$v_d^t = \frac{V}{A_S} \cdot \frac{1}{C_{outlet}^t} \left[\lambda \left(C_{inlet}^t - C_{outlet}^t \right) - L_{bg} \left(\frac{A_{BG} - A_{S,p}}{A_{BG}} \right) C_{outlet}^t - \frac{C_{outlet}^t - C_{outlet}^{t+1}}{\Delta t} \right] \quad (3)$$

where v_d^t is the ozone deposition velocity at time t to the glass plate (cm s^{-1}), V is the volume of the chamber (cm^3), A_s is the area of the top and sides of the glass plate (cm^2), C_{inlet}^t is the ozone concentration entering the chamber at time t (ppb), C_{outlet}^t is the ozone concentration exiting the chamber at time t (ppb), A_{BG} is the area of background chamber surface (cm^2), $A_{S,p}$ is the projected area of the glass plate (cm^2), and all other terms as defined previously.

The total molar uptake of ozone to a test glass plate, Φ (mol), was determined as shown in eq. 4:

$$\Phi = \sum_{t=1}^{n} v_d^t \times \bar{C}_{\Delta t} \times A_S \times \Delta t \quad (4)$$

where $\bar{C}_{\Delta t}$ is the average ozone concentration (mol m^{-3}) in the chamber during the five-minute period, Δt, in which v_d^t is calculated.

Ozone deposition velocities were further parameterized according to resistance-uptake theory, where v_d can be expressed in terms of a transport limited deposition velocity, v_t (cm s^{-1}) and a reaction probability, γ (-), or the fraction of ozone-surface collisions that result in a reaction [14,28,38], shown in eq. 5:

$$\frac{1}{v_d} = \frac{1}{v_t} + \frac{4}{\gamma\langle v\rangle} \quad (5)$$

where $\langle v\rangle$ is the Boltzmann velocity (cm s^{-1}).

The v_t was determined from an experiment in which cleaned glass was coated in a solution of 20 g of potassium iodide (>99% purity, Sigma-Aldrich) dissolved in 25 mL of deionized water. The solution was applied to a cleaned borosilicate glass dish with a small lip. The dish was then dried in the chamber with cleaned, ozone-free air until a solid KI film coated the surface of the dish. An ozone deposition experiment was conducted and the deposition velocity was determined using eq. 2. This condition assumed negligible reaction resistance (i.e., $\frac{4}{\gamma\langle v\rangle} \ll \frac{1}{v_t}$) such that $v_d = v_t$. Since fluid dynamic conditions in the chamber were held constant across all experiments, this allowed determination of γ in subsequent experiments. The experimentally determined v_t ($\mu \pm \sigma = 0.57 \pm 0.028$ cm/s) is shown in Fig. S3 and is in general agreement with previously determined values in laboratory [18] and field environments [39].

To enable statistical comparison across dynamic estimates of ozone reactivity, we employed a metric that characterized the time-variant reaction probability to enable regression analysis. First-order kinetics were applied to the transient values of the reaction probability as shown in equation 6:

$$\frac{d\gamma(t)}{dt} = -\beta \times \gamma(t) \quad (6)$$

where $\gamma(t)$ is the time-varying reaction probability (-), t is the time (min), and β (min^{-1}) is the first-order decay constant of the reaction probability.

With the initial condition of $t = 0$, $\gamma(t) = \gamma(t = 0)$, the solution to eq. 6 takes the form $y = mx$ where y is $-ln\left(\frac{\gamma(t)}{\gamma(t=0)}\right)$, m is β, and x is the time during an experiment where reaction probability is being measured. Higher values of β indicate a faster decay of the reaction probability than lower values of β.

2.6.2 Quality assurance

Experimental uncertainty in estimates of deposition velocities were determined using a propagation of errors analysis for eq. 3, based on the manufacturer's specifications of instrument error. An uncertainty of the greater of 2 ppb or 2% was used for the ozone monitor for inlet and outlet ozone measurements, 1.5% of the reading for the mass flow controller for uncertainty on air exchange, while the error introduced due to area and volume measurements of plates was assumed to be 1%. Uncertainty in calculated reaction probabilities was taken as the sum of the experimental uncertainty for v_d and v_t in quadrature. Reported uncertainties on absolute mass measurements are given as the repeatability of the balance summed in quadrature for two measurements, or ± 0.14 mg. Uncertainties reported for cumulative ozone uptake are reported from a propagation of errors analysis on eq. 4 considering uncertainty on v_d^t and the chamber ozone concentration. The total uncertainty on molar uptake was determined by summing uncertainty at each time step in quadrature.

3. Results and Discussion

3.1 Rates of mass accretion to glass plates

Measurements of total mass accretion to glass plates as a function of time deployed are shown in Fig. 2. The figure shows the absolute mass accreted and indicates a general trend of increasing mass with more time spent in the field. Rates of mass accretion were normalized to the area of the upward facing top of the plate. Note that plates were placed on wire racks to avoid direct contact with actual indoor surfaces and enable testing of O_3 removal both upper and lower surfaces. This protocol resulted in exposure of

267 both the top and bottom of glass plates to air (see Figure S1). In the results presented here, only the top
268 surface and sides were exposed to the ozone deposition test chamber. Given that plates were deployed in a
269 horizontal orientation, and were not processed to remove settled particles, we expect the surface film to be
270 comprised of both settled particles and sorbed organic compounds. However, as will be discussed
271 subsequently, mass accretion rates were normalized to the top area of plates because measured
272 magnitudes are in the range that appears predominantly due to deposition of coarse-mode particles and
273 rates of dustfall [34,36].

274 Weschler and Nazaroff [33] summarize the range of magnitudes of mass accretion of particles and
275 SVOCs to surfaces in models and in previous empirical studies. Their work reports a range of mass
276 accretion rates due to adsorption of gas-phase organics in the range of 30-300 μg/(m^2 d) [33]. This
277 reported rate is approximately 1-2 orders of magnitude lower than the accretion rates observed in this
278 study. Mass accretion rates observed here are in general agreement with the upper limit of the range
279 reported by Weschler and Nazaroff [33] to include deposition of coarse mode particles of 20-9000 μg/(m^2
280 d). For example, after 56 days in the field, glass plates in the MV office and NV residence accreted ~0.50-
281 0.78 g/m^2 of additional mass, or 9000-14,000 μg/(m^2 d). The average mass accretion rate across all
282 collected plates is 10,600 μg/(m^2 d) in the MV office vs. 18,500 μg/(m^2 d) in the NV residence, and a one-
283 tailed t-test comparing higher accretion rates in the NV residences vs. MV office is at the threshold of
284 statistical significance (p = 0.054). The range of mass accretion shown in Figure 2 is also in reasonable
285 agreement with experimental results of dustfall rates in the literature. Edwards et al. [40] reported mean
286 values of 2200 and 3700 μg/(m^2 d) in the summer and winter, respectively, in a study of four homes in
287 New Jersey, USA. In a study of 559 Canadian homes meeting a specified cleaning protocol, the reported
288 median dustfall rate was 10,000 μg/(m^2 d) [41]. Thus, the exposure of the bottom face of the plate likely
289 introduced a small, acceptable error (<3%) to the mass accretion rates determined here.

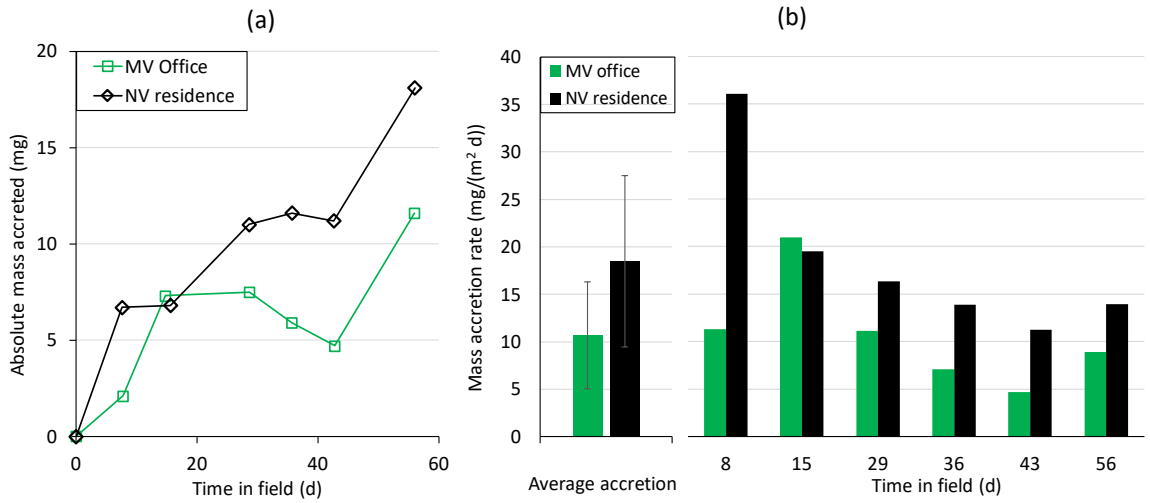

Fig. 2. Summary of mass accretion to test plates in two field environments: mechanically ventilated (MV) office and naturally ventilated (NV) residence. Panel a) shows absolute mass accretion while panel b) shows accretion rates. The average mass accretion rate (mg/(m^2 d)) was calculated as the arithmetic mean of seven mass accretion rates measured over seven weeks. Error bars on average accretion rate are the standard deviation of the mean mass accretion rate. Uncertainty on each estimate of absolute mass accreted is ±0.14 mg as described in the text.

While the mean mass accretion rate in the MV and NV locations are on the threshold of statistical significance in their difference, the magnitude of the difference in all but one sequential measurement of mass accreted to plates in the NV residence is consistently larger than that accreted to the MV office, and greater than the propagated uncertainty in the mass measurement from the analytical balance (i.e., measurement > 0.19 mg). We speculate the consistent difference between the MV and NV plates is due to lack of particle filtration in the NV residence which led to higher indoor particle concentrations and greater deposition flux of particles to the sample surface. Previous studies in Singapore of MV vs. NV residences indicate NV environments have a higher proportion of outdoor particulate matter present indoors than MV environments [42,43].

3.2 Ozone reactivity of plates with accreted mass

3.2.1 Parameterizing transient O_3 removal to surfaces

The deposition of O_3 to indoor surfaces is typically parameterized according to equation 5, where the resistance uptake model ascribes resistances to removal due to transport from a well-mixed bulk core through a concentration boundary layer and subsequent reaction with the surface [27]. Across ozone

deposition experiments, chamber conditions were held constant with the exception of changes in the accreted mass on the glass plate. Therefore, observed changes in v_d can be attributed to the accreted mass present on the glass plate. An illustrative result showing the data collected during an experiment is provided in Figure S4.

As discussed previously in Section 3.1, it appears that the majority of the accreted mass to the glass plates deployed to field environments is derived from deposited particles. Thus, a recent study of ozone reactions occurring on various indoor dust samples [32] provides a relevant basis for comparison for ozone sink strengths. Deposition velocities reported in the first 90 min of each experiment, when observable values are reported, are generally in the range of 0.002-0.025 cm/s across all plates with accreted mass (see Figure S5). These values are roughly consistent with steady-state v_d converted from O_3-dust reaction rates in Vibenholt et al. [32] who report a range of values from 0.008-0.29 cm s^{-1}. We speculate that higher dust loadings in those experiments (1 g vs. ~0.01 g here) explains the generally higher deposition and observation of removal over >12 h time-scales not observed in this study. It is worth noting that v_d reported in both studies are under reaction-limited conditions as the Vibenholt et al. study was conducted in a FLEC cell operated at very high air exchange rate (AER) while for the conditions of this study surface resistance contributes >99% of total resistance for all experiments.

Ozone removal was highest initially and decayed for the duration of the experiment until a steady-state removal indistinguishable from that of background removal was reached. Reaction probabilities for each plate are reported in Table 1; values are arithmetic averages across each hour of the experiment for which γ could be calculated from removal statistically higher than that of the background chamber surfaces. In general, with additional time deployed to the field, reported reaction probabilities increased and O_3 removal persisted for longer periods of testing in the laboratory chamber.

Table 1. Summary of regression parameters and time-averaged reaction probabilities across the first four hours of each experiment of ozone reactivity with deployed plates.

	MV office							NV residence						
	Regression[%]			Rxn. Probability[#], $\gamma\times10^{-6}$				Regression			Rxn. probability, $\gamma\times10^{-6}$			
	β (min^{-1})	**SE $\times10^{-3}$**	**r^2**	**0-1 h**	**1-2 h**	**2-3 h**	**3-4 h**	**β (min^{-1})**	**SE $\times10^{-3}$**	**r^2**	**0-1 h**	**1-2 h**	**2-3 h**	**3-4 h**
0 d	0.045	5.2	0.54	0.74	0.06	-	-	0.045	5.2	0.54	0.74	0.06	-	-
8 d	0.026*	2.9	0.62	0.70	0.01	-	-	0.024*	2.1	0.29	1.0	0.34	0.23	-
15 d	0.020*	1.4	0.62	1.3	0.41	-	-	0.031*	1.9	0.33	1.6	0.43	0.01	-
29 d	0.013*	0.68	0.70	1.1	0.55	-	-	0.0093*	0.46	0.51	1.6	0.76	0.55	0.57
36 d	0.019*	2.0	0.09	1.2	0.38	0.16	-	0.025*	0.61	0.47	1.8	0.82	0.60	0.46
42 d	0.019	1.7	0.35	1.2	0.24	0.06	-	0.013*	0.65	0.67	1.5	0.72	0.46	0.18
56 d	0.018	2.0	0.23	1.2	0.29	0.17	0.15	0.013	0.61	0.75	1.8	0.83	0.48	0.19
Field Blank	0.046	4.7	0.53	1.3	0.07	-	-	0.051	2.5	0.61	1.5	0.08	-	-

[%]Reported regression parameters are the resulting slope, standard error (SE) of the slope, and correlation coefficient from the y = mx linear regression of natural logarithm transformed reaction probabilities.
[#]Reaction probabilities are the arithmetic average across the indicated period of the experiment. Dashes indicate the reaction probabilities were indistinguishable from background removal for that period.
*Indicated values of β are statistically significantly different than the estimate of the preceding plate. Note that slopes for all plates > 0 d are statistically significantly different from the 0 d plate.

In general, the parameterization of the time-variant reaction probability with equation 6 resulted in r^2 values of the regression that were typically >0.5 (see Figure S6 for examples of the regression). Several experiments had low r^2 values (<0.4) but are included in subsequent analyses for completion and to facilitate the goals of the regression analysis to enable statistical comparison across experiments. The analysis of transient decay data also enables determination of the dynamics of ozone reactions to accreted masses that would be obscured by solely comparing the cumulative O_3 removed as in Section 3.2.2. For example, the data reported in Table 1 demonstrate that as larger masses accrete to surfaces, increasing periods of time are required to increase cumulative O_3 removal.

Across plates deployed in both the MV office and the NV residence, values of β decreased as plates were deployed for longer periods. This trend continued until approximately 42 days of deployment (Table 1). From 42-56 days, slopes of the regression appear to stabilize at approximately β = 0.013-0.019. Note that higher values of β indicate the magnitude of γ is "decaying" more rapidly than for lower values of β. This

observation is also observed in that measurable values of γ persisted into 3-4 hours of the experimental testing only for glass plates deployed for 56 d (MV office) or 29 days or greater (NV residence). Statistical significance of differences in β were determined by calculating z-scores from the difference in slopes divided by the difference in the standard error of the slopes of the regression. The detailed procedure is described in the Supporting Information. A summary of *p*-values for comparisons between each plate and the preceding plate, as well as each plate compared to the 0 day plate, are provided in Tables S1 and S2 of the Supporting Information. It appears that surface mass accretion results in significant differences in O_3 reactivity, especially in the first month of deployment. Differences in β are not statistically distinguishable when comparing longer deployment periods for plates deployed in MV offices or NV residences, e.g., the plates deployed for 36 d and 42 d are statistically similar, as are plates deployed for 42 d and 56 d, for the MV office. For the NV residence, the plate deployed for 42 d is similar to the plate deployed for 56 d.

3.2.2 Parameterizing cumulative ozone removal to surfaces with accreted mass

It appears that for glass plates, accretion of mass to the surface of the plate results in a general trend of increasing O_3 reactivity. The relationship between mass accretion and cumulative O_3 removed is explored in Fig. 3, which presents cumulative O_3 removed as a function of mass accreted (panel a) and the average reaction probability as a function of total mass accreted (panel b). The period of 15-200 minutes was selected to calculate the cumulative O_3 removal and the average γ. Cumulative O_3 uptake to the accreted mass is in the range of 20-90 nmol (Figure 3a), with a general increasing trend with greater accreted mass to the plate for both MV and NV environments. Variance in the observed cumulative O_3 removed was similarly and relatively well-explained by the mass accreted to the plate for both MV and NV environments (r^2 = 0.75-0.76).

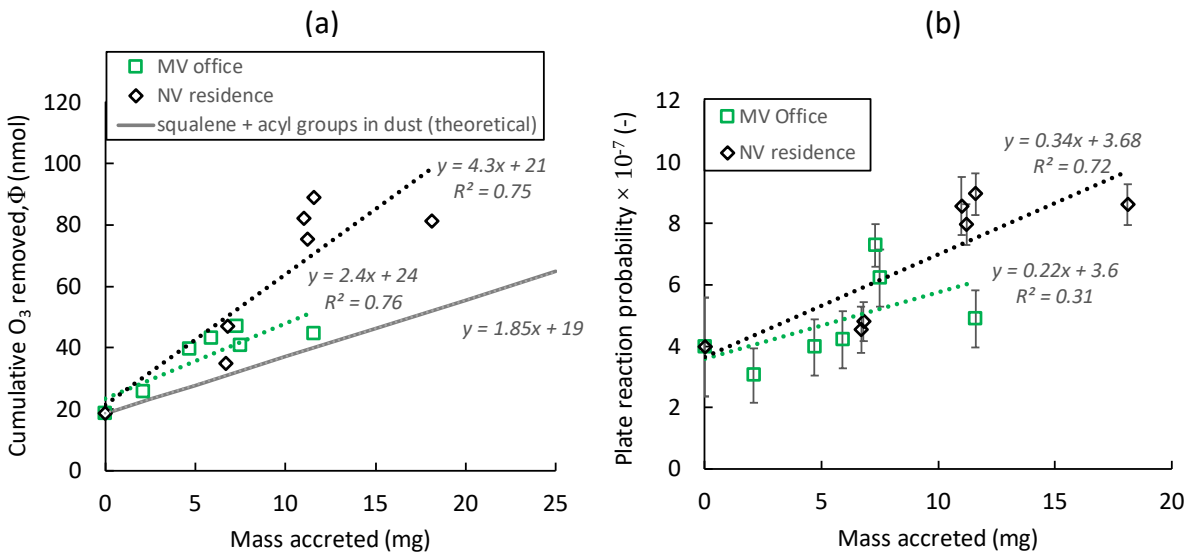

Fig. 3. Panel a) Cumulative O_3 a function of mass accreted to field deployed glass plates. Cumulative uptake is determined from the period 15-200 minutes following the injection of ozone into the chamber. The theoretical uptake from squalene and acyl groups assumes accretion of mass with reaction sites from human-derived constituents onto a surface with the same initial reactivity (that is, 0 mg of accreted mass) as the clean glass plates used in the NV and MV environments. Panel b) Reaction probability as a function of accreted mass.

The slopes shown in Figure 3a provide a proxy for the total reactivity of the accreted surface mass. The intercept is indicative of the reactivity of a clean plate, that is, the plate with no accreted mass from deployment to a field environment. The cumulative O_3 removal to a clean glass plate was 19 nmol. The results shown in Figure 3a indicate that 4.3 nmol O_3 was removed per mg of accreted mass for the NV residence vs. 2.4 nmol O_3 per mg of accreted mass for the MV office. The *p*-values for slopes of the regressions in Figure 3a were statistically significant for both the MV and NV environments ($p = 0.011$ and 0.011, respectively), which together with relatively high r^2 values implies mass accreted is a meaningful predictor of observed changes in cumulative O_3 removal. The data reported in Figure 3a indicate that the mass accreted in the NV residence results in nearly twice the cumulative surface O_3 removal compared to the MV office. However, a comparison of the standard error of the difference between the slopes shown in Figure 3a is calculated and is not statistically significant ($p = 0.13$).

Two pathways are typically considered as mechanisms of O_3 reaction with indoor surfaces. Ozone may react with the accreted mass via catalytic degradation [32] or via the Criegee mechanism at carbon double

bonds present in organic compounds in the accreted mass [5,32,44]. Previous studies, summarized by Weschler [45], show that the presence of humans in indoor spaces results in transfer of skin flakes (desquamation) and skin oils to indoor surfaces. These human-derived constituents contain compounds, namely squalene [46] and acyl groups [47], that may act as O_3 surface reaction sites. The subsequent analysis quantitatively evaluates the extent to which human-derived skin flakes and skin oils may explain the observed removal to accreted mass on glass plates deployed to the MV and NV test environments.

Weschler et al. [48] estimate that dust contains approximately 60 μg of squalene per gram. This is equivalent to 150 nmol of squalene present in each gram of accreted dust. There are six available double bonds in a squalene molecule with which O_3 may react [49]. In addition to squalene, there are other co-occurring compounds present in human skin oil that also contribute unsaturated sites where ozone chemistry can occur. Pandrangi and Morrison [47] estimate that the molar fraction of unsaturations are split between acyl groups (0.48) and squalene (0.44). Combining squalene and acyl groups, there are available unsaturated reaction sites to remove 12.5 nmol of O_3 per nmol of squalene present in dust. Normalizing by the previously noted mass of squalene in dust yields a ratio of ~1.85 nmol of O_3 removal due to squalene and acyl groups for every mg of accreted dust.

The previous estimate of the reactivity of squalene and acyl groups in particles calculated from the literature, 1.85 nmol O_3 removal/mg of accreted mass, can be compared with the reactivity of the accreted mass calculated using equation 4. The theoretical O_3 removal due to squalene and acyl groups in dust is shown in Figure 3a, with the same intercept as a cleaned glass plate. Comparing the slope of the theoretical squalene and acyl groups line with slopes from plates deployed in the two field environments shows that 42% (NV residence) and 75% (MV office) of O_3 may be attributed to these components on human skin oil. Note again that this analysis assumes, as discussed in Section 3.1, that particles or dust are the predominant contributor to the accreted mass observed here.

The calculation of 42-75% of the total removed O_3 as due to skin oil constituents implies other O_3 reactive constituents are also present in the accreting mass. A recent study of heterogeneous oxidation of

squalene with O_3 reported reactive uptake coefficients of $[4.0\text{-}4.3]\times10^{-4}$ [50]. Values of plate reaction probability reported here are much lower, with average values between $[2\text{-}9]\times10^{-7}$ (Figure 3b). We speculate this difference is a result of other compounds present in the accreting mass, as well as a relatively low total accreted mass and potential for oxidation of highly reactive compounds like squalene to occur while aging in the field. A study of the chemical composition of house dust reports total carbon content on the order of 23-33% by mass [51,52]. Metals are shown to be a contributor to the indoor dust composition, e.g., calcium levels of between 5-7% by mass are reported in two studies of the composition of house dust [41,52]. While the form of calcium in dust is not reported, there is precedence in the literature that ozone reactions with, for example, calcium carbonate, will not proceed via irreversible deposition, but rather reversible adsorption [53]. Given that the composition of indoor dust is expected to be highly variable [41], this discussion is speculative and intended to be illustrative of the potential for sources of lower reactivity compounds in masses accreting to indoor surfaces. The need for further study of oxidation on indoor accreted mass paired with chemical composition of the accreted mass is noted.

3.2.3 Study limitations and future directions

It is worth noting that plates were deployed in real field environments with low, but non-zero O_3 concentrations; the O_3 reactivity reported from testing in the laboratory does not account for oxidation reactions that are likely to have occurred while the plates were deployed. Continuous interactions of ozone with indoor surface films while deployed can reduce concentrations of surface unsaturated sites by oxidation. Therefore, the estimates of the reactivity of the surface film reported here are likely underestimating the true reactivity of the accreted mass. It is possible that the indoor concentration of oxidants, rather than a difference in the amount or chemical makeup of the accreted mass, may be the driver of the observed differences in reactivity between the NV residence (no filtration, frequently open windows) and MV office (filters present in HVAC system, windows never open). We parameterized the changing reaction probability using first-order kinetics to enable regression analysis, effectively treating the changing reaction probability as a proxy for the changing density of surface reaction sites. It is

447 possible that these dynamics could be more mechanistically explained if surface concentrations of
448 unsaturated sites in the accreted mass were known.

449 We tested field blanks where cleaned glass plates were deployed inside sealed polypropylene bags for the
450 duration of their deployment to the field. However, we speculate that the mass observed on the field blank
451 plates was unacceptably influenced by water vapor condensing on the plate that penetrated the consumer
452 grade polypropylene storage bag during the deployment. There are limited points of comparison in the
453 literature to either inform or compare the quality assurance measures taken here. In a study of surface
454 films on windows, Liu et al.[34] show that field blank Kimwipes, which were waved in the indoor air of
455 the field environment but were not in contact with the target window, contained 24% of the average
456 sample value of n-alkanes and 1% of the sample concentrations of polar compounds. Wallace et al. [36],
457 who conducted a study using collection methods similar to those described here, investigate the potential
458 for bare hand contact to contaminate surfaces, but do not isolate surfaces to consider as a field blank.
459 Further effort to standardize field sampling methods that use inert surfaces as media for experiments of
460 aging and surface film accretion in indoor spaces is warranted.

461 The findings of this study compel further quantitative research into the study of the reactivity of accreted
462 masses on surfaces as a function of building operation, building type, and indoor air pollution levels.
463 Characterization of surface-bound compounds pre- and post-ozonation would be beneficial in elucidating
464 the specific contributors to O_3 reaction sites in mass accreted to indoor surfaces. There is precedence in
465 the literature for indoor and outdoor derived aerosols to differ in terms of chemical composition [54,55],
466 biological content [56], and water content [54]. Future studies should examine how these factors influence
467 the reactivity of the surface in addition to amount of mass accreted.

468 **4. Conclusions**

469 Accretion of mass to surfaces may alter reaction pathways by providing distinct reaction sites from those
470 of the original material. Previous studies of O_3 removal to materials have used aged building materials in
471 studies, most notably carpet, drywall, and ceiling tile samples [14,18,25]. This study employed an initially

inert, cleaned glass material to provide a baseline that allows isolation of the effect of the accreted mass on surface O_3 reactions. The results show that the accretion of mass to the glass plates resulted in as much as a factor of 4.5 increase in cumulative O_3 surface removal. Ozone reaction probabilities increased with time spent in the field and mass accreted. Notable differences in the cumulative O_3 removed per mass accreted to the surface were observed for plates deployed to MV vs. NV environments, implying building operation may affect how materials interact with indoor O_3. In the range of ~40-70% of total O_3 removal may result from human skin and skin oil constituents present in the accreted mass. Given the large extent of available surface area in indoor environments, further study of aging, mass accretion, oxidation and oxidant cycling, byproduct formation and the integrated effect on indoor air quality and human exposure is warranted.

Acknowledgements

This research was funded by Portland State University start-up funds and the Republic of Singapore's National Research Foundation through a grant to the Berkeley Education Alliance for Research in Singapore (BEARS) for the Singapore-Berkeley Building Efficiency and Sustainability in the Tropics (SinBerBEST) Program. BEARS has been established by the University of California, Berkeley as a center for intellectual excellence in research and education in Singapore.

References

[1] J.L. Peel, M. Klein, W.D. Flanders, J.A. Mulholland, G. Freed, P.E. Tolbert, Ambient air pollution and apnea and bradycardia in high-risk infants on home monitors, Environ. Health Perspect. 119 (2011) 1321–1327. doi:10.1289/ehp.1002739.

[2] I. Romieu, F. Meneses, S. Ruiz, J. Huerta, J.J. Sienra, M. White, R. Etzel, M. Hernandez, Effects of intermittent ozone exposure on peak expiratory flow and respiratory symptoms among asthmatic children in Mexico City, Arch. Environ. Health. 52 (1997) 368–376. doi:10.1080/00039899709602213.

[3] J.I. Levy, S.M. Chemerynski, J.A. Sarnat, Ozone exposure and mortality: "An empiric bayes metaregression analysis," Epidemiology. 16 (2005) 458–468.

[4] J.H. Seinfeld, S.N. Pandis, Atmospheric chemistry and physics: from air pollution to climate change, Wiley, 2006.

[5] C.J. Weschler, Ozone in indoor environments: concentration and chemistry, Indoor Air. 10 (2000) 269–288. doi:10.1034/j.1600-0668.2000.010004269.x.

[6] C. Chen, B. Zhao, C.J. Weschler, Assessing the influence of indoor exposure to "outdoor ozone" on the relationship between ozone and short-term mortality in U.S. communities, Environ. Health Perspect. 120 (2012) 235–240. doi:10.1289/ehp.1103970.

[7] C.J. Weschler, Ozone's impact on public health: contributions from indoor exposures to ozone and products of ozone-initiated chemistry, Environ. Health Perspect. 114 (2006) 1489–1496.

[8] L.J. Liu, P. Koutrakis, H.H. Suh, J.D. Mulik, R.M. Burton, Use of personal measurements for ozone exposure assessment: a pilot study., Environ. Health Perspect. 101 (1993) 318–324.

[9] M.L. Bell, R.D. Peng, F. Dominici, The exposure-response curve for ozone and risk of mortality and the adequacy of current ozone regulations, Environ. Health Perspect. 114 (2006) 532–536.

[10] C.J. Weschler, New directions: Ozone-initiated reaction products indoors may be more harmful than ozone itself, Atmos. Environ. 38 (2004) 5715–5716. doi:10.1016/j.atmosenv.2004.08.001.

[11] D.A. Kunkel, E.T. Gall, J.A. Siegel, A. Novoselac, G.C. Morrison, R.L. Corsi, Passive reduction of human exposure to indoor ozone, Build. Environ. 45 (2010) 445–452. doi:10.1016/j.buildenv.2009.06.024.

[12] E. Darling, G.C. Morrison, R.L. Corsi, Passive removal materials for indoor ozone control, Build. Environ. 106 (2016) 33–44. doi:10.1016/j.buildenv.2016.06.018.

[13] R.H. Sabersky, D.A. Sinema, F.H. Shair, Concentrations, decay rates, and removal of ozone and their relation to establishing clean indoor air, Environ. Sci. Technol. 7 (1973) 347–353. doi:10.1021/es60076a001.

[14] G.C. Morrison, W.W. Nazaroff, The rate of ozone uptake on carpets: Experimental studies, Environ. Sci. Technol. 34 (2000) 4963–4968. doi:10.1021/es001361h.

[15] R. Reiss, P.B. Ryan, P. Koutrakis, S.J. Tibbetts, Ozone reactive chemistry on interior latex paint, Environ. Sci. Technol. 29 (1995) 1906–1912. doi:10.1021/es00008a007.

[16] E.T. Gall, R.L. Corsi, J.A. Siegel, Barriers and opportunities for passive removal of indoor ozone, Atmos. Environ. 45 (2011) 3338–3341. doi:10.1016/j.atmosenv.2011.03.032.

[17] J.G. Klenø, P.A. Clausen, C.J. Weschler, P. Wolkoff, Determination of ozone removal rates by selected building products using the FLEC emission cell, Environ. Sci. Technol. 35 (2001) 2548–2553. doi:10.1021/es000284n.

[18] D. Rim, E.T. Gall, R.L. Maddalena, W.W. Nazaroff, Ozone reaction with interior building materials: Influence of diurnal ozone variation, temperature and humidity, Atmos. Environ. 125, Part A (2016) 15–23. doi:10.1016/j.atmosenv.2015.10.093.

[19] T. Grøntoft, M.R. Raychaudhuri, Compilation of tables of surface deposition velocities for O_3, NO_2 and SO_2 to a range of indoor surfaces, Atmos. Environ. 38 (2004) 533–544. doi:10.1016/j.atmosenv.2003.10.010.

[20] O.A. Abbass, D.J. Sailor, E.T. Gall, Effect of fiber material on ozone removal and carbonyl production from carpets, Atmos. Environ. 148 (2017) 42–48. doi:10.1016/j.atmosenv.2016.10.034.

[21] O.A. Abbass, D.J. Sailor, E.T. Gall, Effectiveness of indoor plants for passive removal of indoor ozone, Build. Environ. 119 (2017) 62–70. doi:10.1016/j.buildenv.2017.04.007.
[22] J. Shen, Z. Gao, Ozone removal on building material surface: A literature review, Build. Environ. 134 (2018) 205–217. doi:10.1016/j.buildenv.2018.02.046.
[23] G.C. Morrison, W.W. Nazaroff, Ozone interactions with carpet: Secondary emissions of aldehydes, Environ. Sci. Technol. 36 (2002) 2185–2192. doi:10.1021/es0113089.
[24] S.P. Lamble, R.L. Corsi, G.C. Morrison, Ozone deposition velocities, reaction probabilities and product yields for green building materials, Atmos. Environ. 45 (2011) 6965–6972. doi:10.1016/j.atmosenv.2011.09.025.
[25] C.J. Cros, G.C. Morrison, J.A. Siegel, R.L. Corsi, Long-term performance of passive materials for removal of ozone from indoor air, Indoor Air. 22 (2012) 43–53. doi:10.1111/j.1600-0668.2011.00734.x.
[26] P. Wolkoff, How to measure and evaluate volatile organic compound emissions from building products. A perspective, Sci. Total Environ. 227 (1999) 197–213. doi:10.1016/S0048-9697(99)00019-4.
[27] W.W. Nazaroff, A.J. Gadgil, C.J. Weschler, Critique of the use of deposition velocity in modeling indoor air quality, in: Model. Indoor Air Qual. Expo. Nagda NL Ed, American Society for Testing and Materials, Philadelphia, 1993. http://www.astm.org/DIGITAL_LIBRARY/STP/PAGES/STP13101S.htm (accessed July 20, 2017).
[28] E.T. Gall, J.A. Siegel, R.L. Corsi, Modeling ozone removal to indoor materials, including the effects of porosity, pore diameter, and thickness, Environ. Sci. Technol. 49 (2015) 4398–4406. doi:10.1021/acs.est.5b00023.
[29] W.W. Nazaroff, G.R. Cass, Mathematical modeling of chemically reactive pollutants in indoor air, Environ. Sci. Technol. 20 (1986) 924–934. doi:10.1021/es00151a012.
[30] R. Reiss, P.B. Ryan, P. Koutrakis, Modeling ozone deposition onto indoor residential surfaces, Environ. Sci. Technol. 28 (1994) 504–513. doi:10.1021/es00052a025.
[31] M.S. Waring, J.R. Wells, Volatile organic compound conversion by ozone, hydroxyl radicals, and nitrate radicals in residential indoor air: Magnitudes and impacts of oxidant sources, Atmos. Environ. 106 (2015) 382–391. doi:10.1016/j.atmosenv.2014.06.062.
[32] A. Vibenholt, P.A. Clausen, P. Wolkoff, Ozone reaction characteristics of indoor floor dust examined in the emission cell “FLEC,” Chemosphere. 107 (2014) 230–239. doi:10.1016/j.chemosphere.2013.12.048.
[33] C.J. Weschler, W.W. Nazaroff, Growth of organic films on indoor surfaces, Indoor Air. 27 (2017) 1101–1112. doi:10.1111/ina.12396.
[34] Q.-T. Liu, R. Chen, B.E. McCarry, M.L. Diamond, B. Bahavar, Characterization of polar organic compounds in the organic film on indoor and outdoor glass windows, Environ. Sci. Technol. 37 (2003) 2340–2349. doi:10.1021/es020848i.
[35] M.L. Diamond, S.E. Gingrich, K. Fertuck, B.E. McCarry, G.A. Stern, B. Billeck, B. Grift, D. Brooker, T.D. Yager, Evidence for organic film on an impervious urban surface: Characterization and potential teratogenic effects, Environ. Sci. Technol. 34 (2000) 2900–2908. doi:10.1021/es9906406.
[36] L.A. Wallace, W.R. Ott, C.J. Weschler, A.C.K. Lai, Desorption of SVOCs from heated surfaces in the form of ultrafine particles, Environ. Sci. Technol. 51 (2017) 1140–1146. doi:10.1021/acs.est.6b03248.
[37] B.K. Coleman, M.M. Lunden, H. Destaillats, W.W. Nazaroff, Secondary organic aerosol from ozone-initiated reactions with terpene-rich household products, Atmos. Environ. 42 (2008) 8234–8245. doi:10.1016/j.atmosenv.2008.07.031.
[38] E.T. Gall, R.L. Corsi, J.A. Siegel, Impact of physical material properties on ozone removal by several porous materials, Environ. Sci. Technol. 48 (2014) 3682–3690. doi:10.1021/es4051956.

589 [39] E. Gall, E. Darling, J.A. Siegel, G.C. Morrison, R.L. Corsi, Evaluation of three common green
590 building materials for ozone removal, and primary and secondary emissions of aldehydes, Atmos.
591 Environ. 77 (2013) 910–918. doi:10.1016/j.atmosenv.2013.06.014.
592 [40] R.D. Edwards, E.J. Yurkow, P.J. Lioy, Seasonal deposition of housedusts onto household surfaces,
593 Sci. Total Environ. 224 (1998) 69–80. doi:10.1016/S0048-9697(98)00348-9.
594 [41] P.E. Rasmussen, C. Levesque, M. Chénier, H.D. Gardner, H. Jones-Otazo, S. Petrovic, Canadian
595 House Dust Study: population-based concentrations, loads and loading rates of arsenic, cadmium,
596 chromium, copper, nickel, lead, and zinc inside urban homes, Sci. Total Environ. 443 (2013) 520–
597 529. doi:10.1016/j.scitotenv.2012.11.003.
598 [42] A. Chen, E.T. Gall, V.W.C. Chang, Indoor and outdoor particulate matter in primary school
599 classrooms with fan-assisted natural ventilation in Singapore, Environ. Sci. Pollut. Res. Int. (2016).
600 doi:10.1007/s11356-016-6826-7.
601 [43] E.T. Gall, A. Chen, V.W.-C. Chang, W.W. Nazaroff, Exposure to particulate matter and ozone of
602 outdoor origin in Singapore, Build. Environ. 93, Part 1 (2015) 3–13.
603 doi:10.1016/j.buildenv.2015.03.027.
604 [44] R. Criegee, Mechanism of Ozonolysis, Angew. Chem.-Int. Ed. Engl. 14 (1975) 745–752.
605 doi:10.1002/anie.197507451.
606 [45] C.J. Weschler, Roles of the human occupant in indoor chemistry, Indoor Air. 26 (2016) 6–24.
607 doi:10.1111/ina.12185.
608 [46] A. Wisthaler, C.J. Weschler, Reactions of ozone with human skin lipids: Sources of carbonyls,
609 dicarbonyls, and hydroxycarbonyls in indoor air, Proc. Natl. Acad. Sci. 107 (2010) 6568–6575.
610 doi:10.1073/pnas.0904498106.
611 [47] L.S. Pandrangi, G.C. Morrison, Ozone interactions with human hair: Ozone uptake rates and
612 product formation, Atmos. Environ. 42 (2008) 5079–5089. doi:10.1016/j.atmosenv.2008.02.009.
613 [48] C.J. Weschler, S. Langer, A. Fischer, G. Bekö, J. Toftum, G. Clausen, Squalene and cholesterol in
614 dust from danish homes and daycare centers, Environ. Sci. Technol. 45 (2011) 3872–3879.
615 doi:10.1021/es103894r.
616 [49] L. Petrick, Y. Dubowski, Heterogeneous oxidation of squalene film by ozone under various indoor
617 conditions, Indoor Air. 19 (2009) 381–391. doi:10.1111/j.1600-0668.2009.00599.x.
618 [50] S. Zhou, M.W. Forbes, Y. Katrib, J.P.D. Abbatt, Rapid Oxidation of Skin Oil by Ozone, Environ.
619 Sci. Technol. Lett. 3 (2016) 170–174. doi:10.1021/acs.estlett.6b00086.
620 [51] L. Mølhave, T. Schneider, S.K. Kjærgaard, L. Larsen, S. Norn, O. Jørgensen, House dust in seven
621 Danish offices, Atmos. Environ. 34 (2000) 4767–4779. doi:10.1016/S1352-2310(00)00104-7.
622 [52] C. Lanzerstorfer, Variations in the composition of house dust by particle size, J. Environ. Sci.
623 Health Part A. 52 (2017) 770–777. doi:10.1080/10934529.2017.1303316.
624 [53] L. Li, Z.M. Chen, Y.H. Zhang, T. Zhu, J.L. Li, J. Ding, Kinetics and mechanism of heterogeneous
625 oxidation of sulfur dioxide by ozone on surface of calcium carbonate, Atmos Chem Phys. 6 (2006)
626 2453–2464. doi:10.5194/acp-6-2453-2006.
627 [54] A.M. Johnson, M.S. Waring, P.F. DeCarlo, Real-time transformation of outdoor aerosol
628 components upon transport indoors measured with aerosol mass spectrometry, Indoor Air. 27
629 (2017) 230–240. doi:10.1111/ina.12299.
630 [55] R. Balasubramanian, S.S. Lee, Characteristics of indoor aerosols in residential homes in urban
631 locations: a case study in Singapore, J. Air Waste Manag. Assoc. 1995. 57 (2007) 981–990.
632 [56] T. Lee, S.A. Grinshpun, D. Martuzevicius, A. Adhikari, C.M. Crawford, J. Luo, T. Reponen,
633 Relationship between indoor and outdoor bioaerosols collected with a button inhalable aerosol
634 sampler in urban homes, Indoor Air. 16 (2006) 37–47. doi:10.1111/j.1600-0668.2005.00396.x.
635